VI International Conference on Computational Methods in Marine Engineering
MARINE 2015
F. Salvatore, R. Broglia and R. Muscari (Eds)

FREE RUNNING PREDICTION OF A FULLY APPENDED SUBMARINE: EFFECTS OF STERN PLANE CONFIGURATIONS

R. BROGLIA[*], M. CANNAROZZO[†], G. DUBBIOSO[*] AND S. ZAGHI[*]

[*] Maritime Technology Research Centre (CNR-INSEAN)
National Research Council
Via di Vallerano, 128, 00139 Rome, Italy
e-mail: riccardo.broglia@cnr.it

[†] Directorate for Naval Armaments - Submarines (NAVARM)
General Secretariat of Defence
Programme Office, Rome, Italy
email: maurizio.cannarozzo@marina.difesa.it

Key words: Submarines; CFD; Prediction of Trajectory, Free Running.

Abstract. In this paper numerical computations dedicated to the analysis of the maneuvering behavior of a fully appended submarine are presented. The work presented here is part of the CNR-INSEAN activities scheduled in the framework of a joint Italian and Norwegian MoDs project, with the partnership of MARINTEK, under the *egida* of the European Defence Agency. The aim of the project is to exploit the effect of cruciform and X rudder configuration on the turning qualities of the submarine in two operation conditions, namely open water and snorkeling depth. In this paper, the free running turning circle maneuver in open water condition is analyzed; predictions are achieved by an in-house CFD solver.

1 INTRODUCTION

The prediction of the manoeuvring behaviour of a submarine vehicle is usually achieved by means of simplified manoeuvring mathematical models. Broadly accepted mathematical models describing a submarine manoeuvring performance are based on the traditional approach of Gertler and Hagen [1], later on modified by Feldman [2] in order to account for the typical phenomenon characterising the submarine dynamic response, namely the cross coupling effect between yaw and heave-pitch motions. These tools are extremely efficient and fast from the computational point of view because the forcing terms of the Euler rigid body equations, or alternatively, forces and moments acting on the body, are prescribed by means of hydrodynamic derivatives; in other words, hydrodynamic derivatives synthetize hydrodynamic loads acting on a body during a general motion. The success of these tools is strictly dependent on the reliability of the procedure followed for the evaluation of hydrodynamic coefficients. In case of a submarine, derivatives are evaluated ad-hoc case by case, due to critical operational task required for these vehicles.

It has to be emphasized that typical operational requirements of these vehicles are littoral surveillance and, of course, they're necessitate to sail near the free surface at "periscope depth" [3]. In these circumstances, the presence of the boundaries (free surface or bottom) can affect noticeably the vehicle manoeuvring response and, if not properly controlled, compromise its operational tasks. Moreover, new asymmetric threats require modern

submarines to be able not only to ASW and ASuW roles in open water, but also to ISR, SPECOPs and complete integration with other assets in littoral scenarios, exactly where they're necessitate to sail near the free surface at "periscope depth" [3].

In this operational background, the Italian General Secretariat of Defence has been supporting and co-funding research projects on submarines maneuverability since 2003 (see for example [4]), previously with EUCLID (European Cooperation for Long Term in Defence) SUBMOTION and now with EDA (European Defence Agency) SUBMOTION 2, in pursuit of improvement in:

- **tactic:** looking for maneuver training simulators motions laws even more realistic;
- **technique:** accurate and reliable CFD predictions in the early stages of design process can reduce the need for physical prototypes to optimize maneuverability (choosing X or cross rudders, for example), in turn greatly accelerating development process and cutting costs of future submarines;
- **procedures:** enhancing the maneuvering prediction methods in confined waters to provide guidance to operators of existing submarines.

The principal aim of present research is to develop a reliable and practical procedure for the analysis of submarine maneuvering qualities while operating in different operative scenarios (open water, confined motions, escape or emergency maneuvers). In the present paper results of the free running, turning circle simulations are presented and discussed. Cross rudder and X-rudder configurations, sailing in open water are investigated.

In case of the cross rudder configuration the turning maneuver was performed at the maximum rudder angle tested during the experiments performed at QinetiQ in the framework of the Submotion I project [15], namely δ=15°. No experimental data are available for the X-rudder configuration; anyhow, two different rudder angles were tested δ=5°, 10°. Comparison with the cross rudder configuration allows to approximately identifying the equivalent rudder angle that should be prescribed to the X-rudder configuration in order to perform a maneuver similar to the cross rudder.

Computations were carried out on two different grid levels to provide a grid study; results are validated with the experiments in case of the cross rudder configuration only, both in deep and close to free surface conditions. It is worth to note that the motion of the submarine is free on the horizontal plane only; consequently, the inevitable sinking motion experienced by the submarine during the turn owing to the circulation generated by the sail and the cross-coupling of the sway, yaw and roll is not accounted for. This choice seems a plausible assumption, the experiments being carried out keeping the depth fixed by means of an ad-hoc closed loop control system. Simulations have been carried out using the CNR-INSEAN in-house finite volume solver, χnavis. The effect of the propeller is modeled by an actuator disk.

2 NUMERICAL SETUP

The CFD code solves the Navier-Stokes Equations for unsteady high Reynolds number (turbulent) free surface flows around complex geometries. The numerical solution of the governing equations is computed by means of the solver χnavis, which is a general purpose simulation code developed at CNR-INSEAN; the code yields the numerical solution of the unsteady Reynolds averaged Navier Stokes equations for unsteady high Reynolds number

(turbulent) free surface flows around complex geometries (the interested reader is referred to [5]-[10] for details). The solver is based on a finite volume formulation with conservative variables co-located at cell centre. The spatial discretization of the convective terms is done with a third order upwind based scheme, whereas the diffusive terms are discretized with second order centred scheme and the time integration is done by second order implicit scheme (three points backward). The solution at each time step is computed iteratively by a pseudo-time integration that exploits an Euler implicit scheme with approximate factorization, local pseudo time step and multi-grid acceleration [11]. Although several turbulence models have been implemented in the code, in all the simulations reported the turbulent viscosity has been calculated by means of the one-equation model of Spalart and Allmaras [12]. Free surface effects are taken into account by a single phase level-set algorithm [6]. Complex geometries and multiple bodies in relative motion are handled by a dynamical overlapping grid approach [8]. High performance computing is achieved by an efficient shared and distributed memory parallelization [9] and [10].

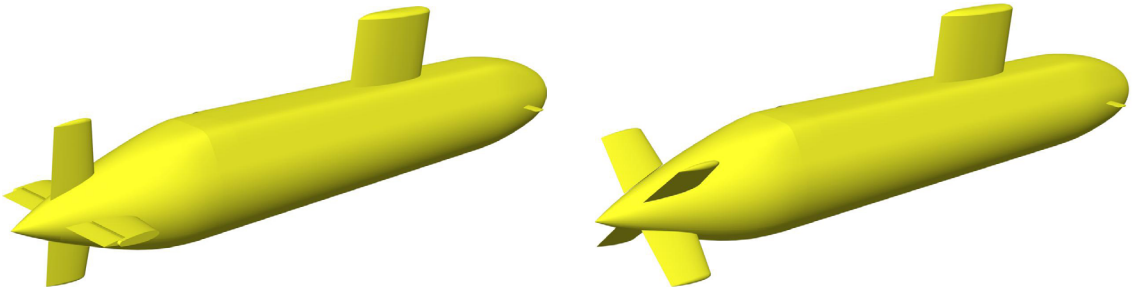

Figure 1: Submarine CNR-INSEAN 2475 model. Left, cruciform rudder; right, X rudder.

3 GEOMETRY AND TEST PARAMETERS

Numerical simulations have been carried out for the submarine chosen within the project (CNR-INSEAN 2475 model), see Figure 1. The model is fully appended with forward planes, the sail, and the stern appendages (rudders). The model is propelled by a seven blades propeller; in the numerical simulations the effect of the propeller is taken into account by means of the modified Hough and Ordway model, supplemented with an estimation of the lateral forces.

In the following, all the quantities are made non dimensional using the length of the main body and the advancement speed at model scale. The corresponding Reynolds and Froude numbers are Re=6.65 10^6 and Fr=0.21, respectively. Two different configurations have been tested, the original cruciform layout and a new X configuration; the rudder geometry was designed maintaining the same total rudder area of the C–rudder configuration in order to first assess a comparison about the course keeping qualities (i.e. directional stability).

3.1 Computational mesh

An overview of the computational mesh (only the surface mesh is shown) is reported in Figure 2; in the figure, chimera cells have been hidden for the sake of clarity. The computational grid used consists of structured patched and overlapped blocks. The total

number of volumes is about 11.8 and 10.5 million for the cross and the X rudder configuration, respectively. Grid distribution is such that the thickness of the first cell on the wall is always below 1 in terms of wall units, i.e. no wall functions have been used.

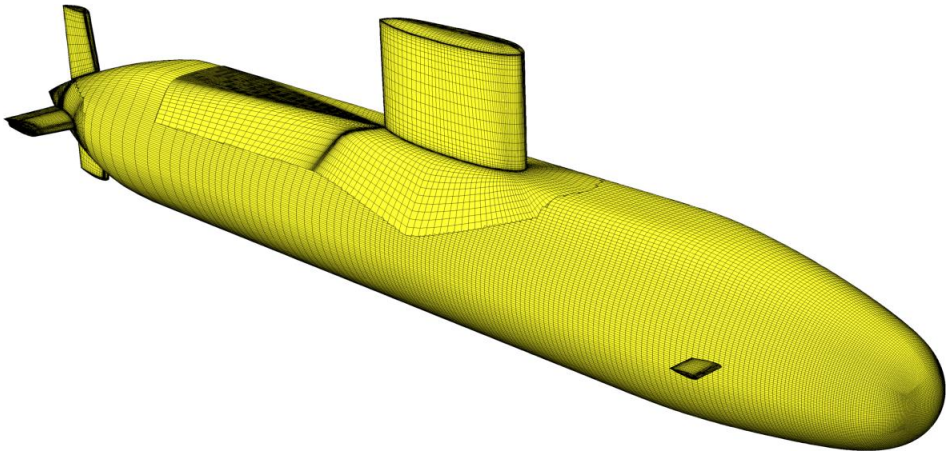

Figure 2 : Surface mesh for the C rudder configuration.

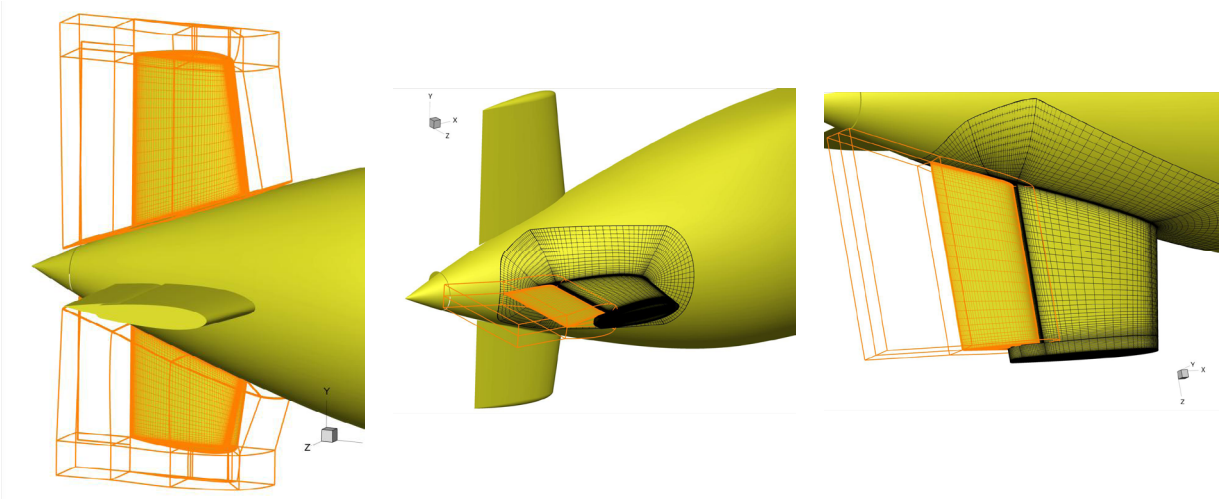

Figure 3: Discretization details of the stern plane.

The inclusion of the appendages is achieved by means of a Chimera approach; the relative motion of the different topologies is achieved by means of a dynamical overlapping grid algorithm (e.g. see Figure 3 where a detail of the stern flap grids is reported). Size and position of the structured blocks in the domain are listed in Table 1 for both configurations. A multigrid technique is exploited in order to achieve a faster convergence to the solution in the pseudo-time; four levels of computational mesh are used. Every level is obtained from the finer one, by removing every other point along each spatial direction.

Table 1: Overlapping blocks: details of the discretization.

Conf.	Zone	No. Blocks	Cells
C and X	Background	2	1.2M
	Hull	84	3.6M
	Sail	34	1.0M
	Bow Plane	88	1.9M
	Actuator disk	1	0.3M
C	Rudder Up	56	0.7M
	Rudder Down	56	0.7M
	Stern Planes Fixed	62	1.8M
	Stern Planes Mobile	64	0.9M
X	Rudder (each)	56	0.7M

3.2 Set-up of free running manoeuvres

The turning circle manoeuvre is carried out at constant propeller rotational speed. The complete simulation is characterized by the following phases:

- **Acceleration:** the model is accelerated from the rest for one non-dimensional time unit. An additional fictitious pushing force (equal in magnitude to the weight of the model) is added to reduce the transient phase. The propeller thrust is switched-off during this phase.
- **Self propulsion and Stabilisation:** the fictitious pushing force is removed and a time accurate self propulsion simulation is performed in order to achieve the true self--propulsion point of the submarine;during this phase, the propeller RPM are continuously adjusted by a PI (proportional-integral controller) until the prescribed approach speed (i.e. Fr=0.21) is obtained. In order to prevent the onset of non-zero yaw rate and drift angle at the start of the manoeuvre (the propeller induces an asymmetric flow around the rudders and the propeller cone and therefore, the generation of an undesired lateral force applied at the stern, i.e. the so-called "Hovgaard effect"), all the motions are restrained but the surge.
- **Free running phase:** once the attitude of the ship has reached a reasonable stable condition, the rudder is rotated with the prescribed turning rate up to the desired angle. During this phase a time resolved simulation is carried out; yaw, sway and surge motions are free, whereas, heave, pitch and roll motions are restrained (i.e. a 3DoF simulation is performed). The simulations are carried out for the time required by the submarine to complete, at least, one complete turns plus and additional (at least) three quarters of turn.

4 NUMERICAL RESULTS

In this paragraph the predictions of the numerical solver are presented for the C and X rudder configuration sailing in infinite depth (open water, OW). The analysis aims to systematically investigate the effect of the control surface configuration. In Table 2 the test matrix is summarized; in order to provide a grid study, free running maneuvers were carried

out both on the reference (F) and a coarser (C) grid obtained by removing every other point along each coordinate.

Table 2: Test Matrix

Configuration	Maneuver	Condition	Grid
C	*Turning δ=15°*	OW	C,F
X	*Turning δ=5°*	OW	C,F
	Turning δ=10°	OW	C,F

It has to be pointed out that in case of the X-rudder configuration experimental free running maneuvering tests are not available, this configuration being exploratory in the present Research Project; in order to grasp an equivalent turning performance to the C rudder, two different rudder angles were considered in order to identify an equivalent control surface angle to perform a direct comparison between the two control surface arrangements.

The maneuvering performance is evaluated in terms of typical macroscopic maneuvering parameters traditionally adopted in ship maneuvering, as well as kinematic parameter experienced during the steady phase of the turn; namely: advance (ADV), transfer (TRA), tactical diameter (TAD), turning radius (TCD), yaw rate, speed drop (during the steady phase) and drift angle.

In order to investigate the reliability of the CFD predictions, a comparison in term of final diameter is made with available results from manoeuvring a mathematical model Cetena [16] and experimental results from QinetiQ [15].

4.1 Manoeuvring Analysis

In Table 3 and Table 4 the results of the turning circle maneuvers are summarized for the C- and X-rudder configurations in terms of trajectory and kinematics parameters. Values refer to the coarse and fine grids adopted; the extrapolate value is obtained by the classical Richardson extrapolation, whereas, the numerical uncertainty U_{SN} (expressed as percentage of the extrapolated value) is evaluated following the procedure of Roache [16] for two grids.

In general, the X-rudder configuration is characterized by better turning qualities with respect to the C-rudder configuration. This is evidenced by the fact that a similar response to the C-rudder configuration is achieved with a 25% reduction of the rudder angle (i.e. □=10°). This behavior is consequent to the criteria adopted to design the novel configuration: the rudder geometry was designed maintaining the same total rudder area of the C--rudder configuration in order to first assess a comparison about the course keeping qualities (i.e. directional stability). In case of the X-rudder configuration, the effective (movable) area is greater with respect to the C configuration (all 4 rudders are deflected) and, consequently, a larger maneuvering (destabilizing) lateral force is exerted to the submarine.

In order to stress the comparison between the two configurations, in Figure 4 both trajectories and time-histories of the kinematic parameters (axial velocity, drift angle and yaw speeds) are shown; the data considered refer to the results obtained on the finest mesh. The matching between the trajectories at δ=15° (C-rudder) and δ=10° (X-rudder) as well as the kinematic response confirms the synthesized results in Table 3 and Table 4.

Table 3: Trajectory parameters, including grid refinement study.

Conf.	Man.	Grid	ADV	TRA	DTAC	DFIN
C	*δ=15°*	C	2.83	1.35	2.97	3.01
		F	2.72	1.35	3.00	3.02
		Extr.	2.68	1.35	3.01	3.02
		U_{SN}%	1.40%	0.00%	0.33%	0.11%
X	*δ=5°*	C	4.06	2.09	4.15	3.86
		F	3.91	2.00	4.09	3.83
		Extr.	3.86	1.97	4.07	3.82
		U_{SN}%	1.36%	1.57%	0.50%	0.26%
	δ=10°	C	2.77	1.28	2.72	2.64
		F	2.62	1.12	2.63	2.61
		Extr.	2.57	1.07	2.60	2.60
		U_{SN}%	2.02%	5.56%	1.18%	0.39%

Table 4: Kinematic parameters, including grid refinement study.

Conf.	Man.	Grid	u/u0	r [deg/s]	Drift [deg]
C	*δ=15°*	C	0.66	7.04	10.01
		F	0.70	7.49	9.70
		Extr.	0.72	7.64	9.60
		U_{SN}%	1.92%	1.89%	1.10%
X	*δ=5°*	C	0.74	6.17	7.94
		F	0.79	6.67	7.80
		Extr.	0.82	6.84	7.75
		U_{SN}%	1.98%	2.32%	0.61%
	δ=10°	C	0.62	7.53	11.12
		F	0.65	8.01	11.01
		Extr.	0.66	8.17	10.97
		U_{SN}%	1.47%	1.88%	0.34%

Good grid convergences are inferred from the general very low numerical uncertainty. The effect of grid refinement is more evident for the trajectory parameters in the transient phase of the maneuver; in general, the numerical uncertainty of the ADV and the TRA is not higher than 2% and 5%, respectively (maximum values are observed for the tighter maneuver, i.e. δ=10°, with the X-rudder configuration). On the contrary, both trajectory and kinematic parameters relative to the stabilized phase show a negligible numerical uncertainty lower than 1% (see DFIN in Table 3) and 2% (Table 4), respectively.

Refining the grid the ADV and the TRA parameters are noticeably reduced for both configurations (i.e., a more reactive response to the rudder control force is predicted when refining the grid). Moreover, the faster reduction of the speed drop (i.e. u/u0) and, on the

other hand, the increase of drift angle and yaw rate immediately after the actuation of the rudder, further highlight as a less stable vehicle is predicted when increasing the grid refinement.

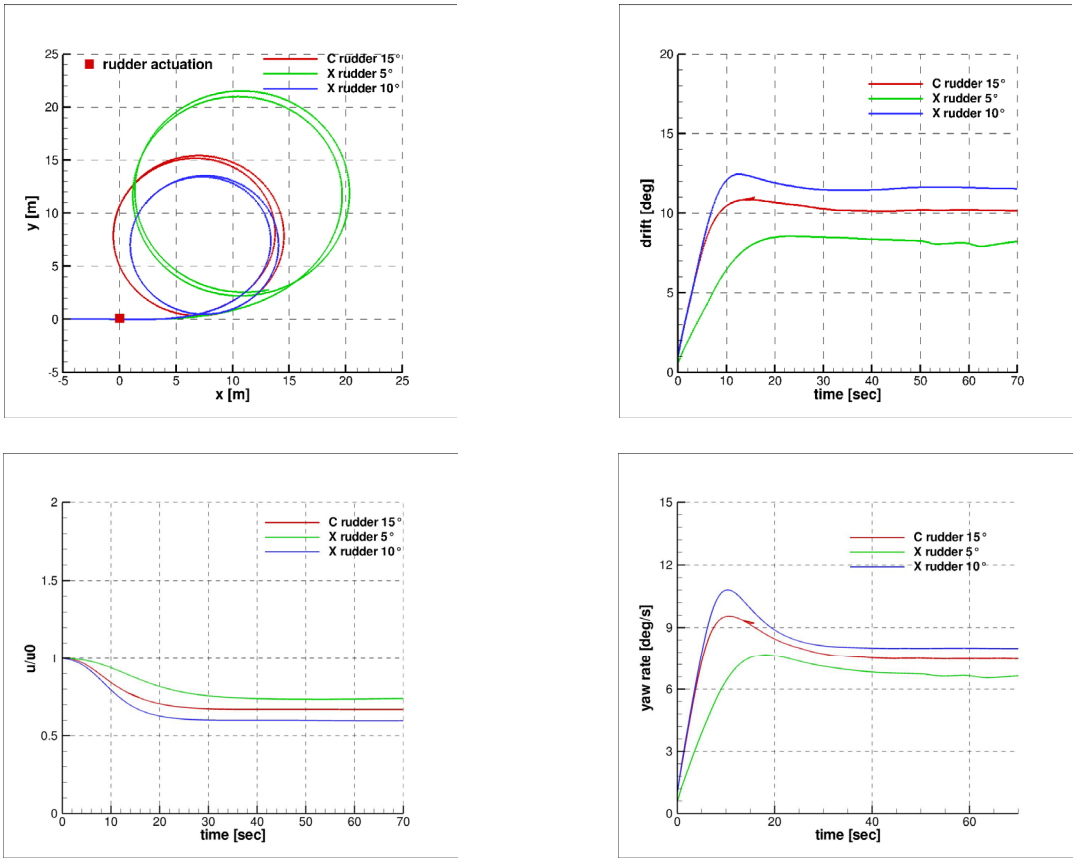

Figure 4: Submarine response in terms of trajectory and kinematics. Comparison between C- and X-rudder configurations. Finest mesh.

Table 5: Final diameter comparison with respect to experiments and regression based models. Final diameter is in meter at model scale (L_{PP}=4.95m).

	EXP	**CFD**	**CET**
DFIN [m]	17.06	14.95	18.01
Δ%	-	-12.43%	5.57%

In Table 5 numerical results (i.e. the extrapolated value) of the C-rudder configuration are compared with the available experimental data and those gathered with two simplified maneuvering mathematical model performed by Cetena (CET) in terms of final diameter.

The final diameter predicted by the CFD simulation is in good agreement with both experiments and CET simulation (differences are about 12% and 15%, respectively).

4.2 Flow field analysis

A global overview of distribution of the pressure field during the steady phase of the turn is shown in Figure 5 for the C- (δ=15°) and X-rudder (δ=10°) configuration. The results correspond to the finest grid level. For the sake of comprehension, the submarine is turning port-to-starboard side and the incoming flow (relative to the body) is directed from right to left, accordingly. A relatively large stagnation region is observed around the nose; immediately downstream, the pressure drops. In the forward portion of the body (approximately $0.15L_{PP}$ from the nose) the pressure levels on the wind side (i.e. right side viewing the submarine from the bow to the stern) seem higher than the lee side. This is consistent to the fact that the resultant force acts in the forward part of the body and is directed toward to the center of the turn.

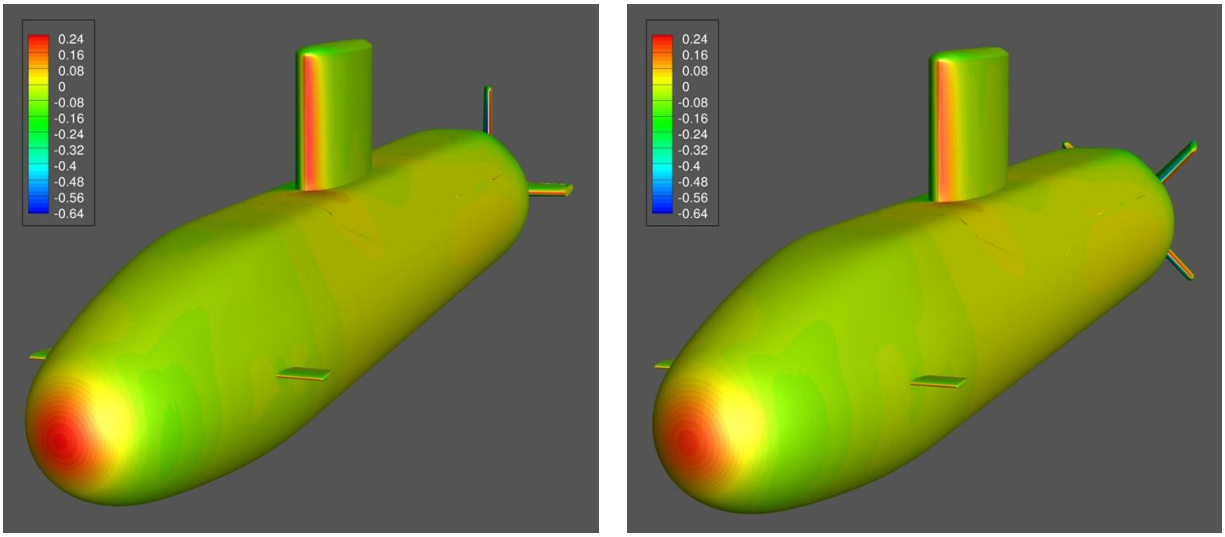

a) C-rudder configuration *δ=15°* b) X-rudder configuration *δ=10°*

Figure 5: Pressure field on hull and control surfaces.

The flow impinges the sail with an incidence angle, as it can be evidenced by the stagnation region over the wind portion of the leading edge; as a consequence, the sail behaves like a small aspect ratio wing and develops lift directed from the wind to the lee side. A similar distribution can be glimpsed over the rudders in case of both configurations; it is seen that a stabilizing effect is provided by the control surfaces. A zoomed views of the pressure field around the rudders is reported in Figure 6 for the C and X configuration, respectively; in case of the X-rudder configuration, the performance of the rudders can be affected by interference with sail and the wake of the hull, as it can be clearly observed by the different extent of the stagnation region for the windward and leeward rudder positioned over the upper half of the submarine.

Finally, a further consideration has to be pointed out on the contribution of the stern rudder during the maneuver: after their actuation, the rudders provide a destabilizing effect, i.e. the force is directed from the lee to the wind side; the hull progressively attains an incidence with respect to the flow and the pressure distribution that develops over the body is such to sustain

the turn of the submarine. The lateral and rotational velocity progressively increase while the effective incidence angle of the rudders diminishes and then changes sign (this is inevitable because up to this moment there is not any contribution that opposes to the turning motion); in this new hydrodynamic condition, the rudders exert a stabilizing effect that counteracts the (opposite) hydrodynamic moment developed by the hull. When the two contributions are close to each other, the equilibrium is achieved and the steady turn establishes.

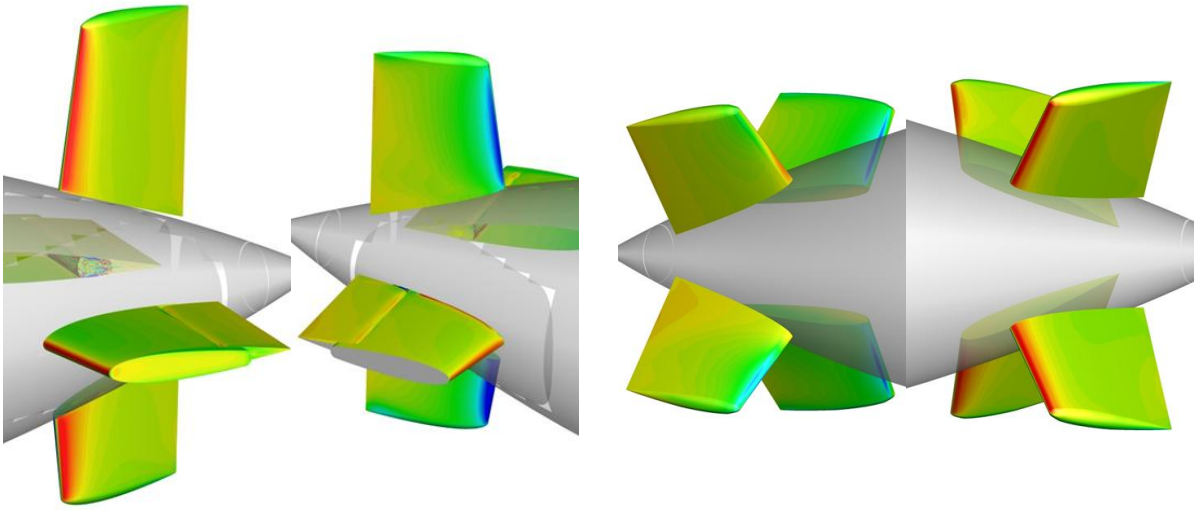

a) C-rudder configuration $\delta=15°$ b) X-rudder configuration $\delta=10°$

Figure 6: Pressure field on rudders; open water condition.

5 CONCLUSIONS

The turning qualities of the submarine model equipped with the two different rudder configurations (cross and X) were investigated by means of numerical simulations. In particular, free running model tests were carried out by the CNR-INSEAN in-house general purpose χnavis solver. The analysis allowed examining many aspects related to the maneuvering prediction of a submarine vehicle, related on both phenomenological and numerical aspects. In particular:

- Capabilities of CFD solver based on the discretization of the unsteady Reynolds-Averaged Navier-Stokes equations in accurately reproduce the turning circle maneuver of a fully appended submarine have been demonstrated. The tool is also able to distinguish between two different stern appendages configurations without making use of any empiricism. The quality of the provided results has been proved by the good convergence properties and the very low numerical uncertainty. A partial validation of the numerical computations was carried out on the C-rudder configuration. The comparison in terms of the final diameter was very satisfactory, the error being of the order of 10% both in the deep water and close to free surface condition.
- The turning qualities of the X-rudder configuration is superior with respect to the original one, principally because the movable area is larger; further studies are necessary to

compare the realistic performance of the new configuration with during a realistic 6DoF simulation to better understand complex interaction phenomena due to hydrodynamic interference with the wake of the hull and the sail (as well as the interaction with coherent structures detaching from other parts of the body), as evidenced by the different pressure field distributions.

- For the condition investigated, the rudder acts as a fixed appendage during the steady turning phase; this phenomenological behavior might be different from that characterizing the maneuvering response of surface vessel. Moreover, in this regard, a direct comparison between the hydrodynamic loads derived by CFD and those physically prescribed in System Based approaches can provide useful suggestion and guidelines for the improvement of simplified maneuvering modeling codes extensively applied in the preliminary design of a submarine.

6 AWKNOWLEDGEMENTS

This work has been supported by the Research Project “Submarine Coupled 6DoF Motions Including Boundary Effects”, SUBMOTION II, financially supported by the Italian and the Norwegian MoDs, contracted through the European Defense Agency.

REFERENCES

[1] Gertler, M., Hagen, G.R., “Standard equations of motion for Submarine Simulation”, 1967, REPORT NSRDC 2510

[2] Feldman J., “Revised Standard Submarine Equations of Motion”, 1979, REPORT DTNSRDC/SPD-0393-39

[3] Burcher, R., Rydill, L., “Concept in Submarine Design”[M], 1994, Cambridge Ocean Technology Series 2.

[4] Broglia, R., Di Mascio A., Muscari, R., ”Numerical Study of Confined Water Effects on Self Propelled Sibmarine in Steady Manoeuvres” [J], IJOPE, Vol.17, No 48, 89-96.

[5] Di Mascio A., Broglia R. Favini, B., 2001, “A second order Godunov-type scheme for naval hydrodynamics, in: Godunov Methods: Theory and Applications”, Kluwer Academic/Plenum Publishers. pp. 253–261.

[6] Di Mascio A., Broglia R. and Muscari R., 2007, “On the application of the single-phase level set method to naval hydrodynamic flows”, Computers & Fluids 36, 868–886.

[7] Di Mascio, A., Broglia, R., and Muscari, R. (2009). “Prediction of hydrodynamic coefficients of ship hulls by high-order Godunov-type methods”. J. Marine Sci. Tech., Vol. 14, pag. 19-29.

[8] Di Mascio, A., Muscari, R., and Broglia, R. (2006). “An Overlapping Grids Approach for Moving Bodies Problems”. 16th ISOPE, San Francisco, California (USA).

[9] Broglia R., Di Mascio A., Amati, G., 2007. “A Parallel Unsteady RANS Code for the Numerical Simulations of Free Surface Flows”, Proc. of 2nd International Conference on Marine Research and Transportation, Ischia, Naples, Italy.

[10] Broglia, R., Zaghi, S., Muscari, R., and Salvadore, F. (July 2014). Enabling hydrodynamics solver for e□cient parallel simulations. In Proc. International Conference on High Performance Computing & Simulation (HPCS), pages 803–810, Bologna, Italy.

[11] Favini, B., Broglia, R., and Di Mascio, A. (1996). “Multigrid Acceleration of Second

Order ENO Schemes from Low Subsonic to High Supersonic Flows". Int. J. Num. Meth. Fluids, vol. 23, pag. 589-606.
[12] Spalart P.R. and Allmaras S.R., "A One-Equation Turbulence Model for Aerodynamic Flows", La Recherche Aerospatiale 1 (1994) 5-21.
[13] Broglia, R., Dubbioso, G., La Gala, F., Santic, F. and Sellini, M., (2013). CNR-INSEAN Technical Report: WP-1.1: Studies on a submarine with fixed and moving appendages: measurement of global and appendage loads.
[14] Watt, G.D., "Estimates for the added mass of a multi component, deeply submerged vehicle", 1988, DREA Technical Memorandum 88/213.
[15] Kimber, N.I. Submarine motions in confined waters - EUCLID RTP 10.17 Free-maneuvering model experiments (Work Element 1.3), 2006. QinetiQ/06/01419.
[16] C. Notaro and J. Labanti. Submotion II –WP3 - Simulation tools. Improvement of simulator models using data from WP1., 2015. CETENA TR 12131.
[17] Roache, P. J. (1997). Quantification of Uncertainty in Computational Fluid Dynamics. Ann. Rev. Fluid Mech., 29:123–160.